frontiers | Frontiers in Physics

TYPE Original Research
PUBLISHED 30 July 2024
DOI 10.3389/fphy.2024.1422286

OPEN ACCESS

EDITED BY
Peter Manz,
University of Greifswald, Germany

REVIEWED BY
Aaro Järvinen,
VTT Technical Research Centre of Finland Ltd., Finland
Dieter Boeyaert,
University of Wisconsin-Madison, United States

*CORRESPONDENCE
L. De Gianni,
ludovica.degianni@cea.fr

RECEIVED 23 April 2024
ACCEPTED 10 June 2024
PUBLISHED 30 July 2024

CITATION
De Gianni L, Ciraolo G, Giruzzi G, Falchetto G, Rivals N, Gałązka K, Balbinot L, Varadarajan N, Sureshkumar S, Artaud JF, Bufferand H, Düll R, Gallo A, Ghendrih P, Quadri V, Rubino G and Tamain P (2024), Core and edge modeling of JT-60SA H-mode highly radiative scenarios using SOLEDGE3X–EIRENE and METIS codes. *Front. Phys.* 12:1422286.
doi: 10.3389/fphy.2024.1422286

Core and edge modeling of JT-60SA H-mode highly radiative scenarios using SOLEDGE3X–EIRENE and METIS codes

L. De Gianni[1]*, G. Ciraolo[1], G. Giruzzi[1], G. Falchetto[1], N. Rivals[1], K. Gałązka[1,2], L. Balbinot[3], N. Varadarajan[1], S. Sureshkumar[1], J. F. Artaud[1], H. Bufferand[1], R. Düll[1], A. Gallo[1], P. Ghendrih[1], V. Quadri[1], G. Rubino[4] and P. Tamain[1]

[1]CEA, IRFM, Saint-Paul-lez-Durance, France, [2]IFPILM, Warszawa, Poland, [3]DEIm Department, University of Tuscia, Viterbo, Italy, [4]ISTP, CNR—Institute for Plasma Science and Technology, Bari, Italy

In its first phase of exploitation, JT-60SA will be equipped with an inertially cooled divertor, which can sustain heat loads of 10 MW/m^2 on the targets for a few seconds, which is much shorter than the intended discharge duration. Therefore, in order to maximize the duration of discharges, it is crucial to develop operational scenarios with a high radiated fraction in the plasma edge region without unacceptably compromising the scenario performance. In this study, the core and edge conditions of unseeded and neon-seeded deuterium H-mode scenarios in JT-60SA were investigated using METIS and SOLEDGE3X–EIRENE codes. The aim was to determine whether, and under which operational conditions, it would be possible to achieve heat loads at the targets significantly lower than 10 MW/m^2 and potentially establish a divertor-detached regime while keeping favorable plasma core conditions. In first analysis, an investigation of the edge parameter space of unseeded scenarios was carried out. Simulations at an intermediate edge power of 15 MW indicate that, without seeded impurities, the heat loads at the targets are higher than 10 MW/m^2 in attached cases, and achieving detachment is challenging, requiring upstream electron densities at least above 4×10^{19} m^{-3}. This points toward the need for impurity injection during the first period of exploitation of the machine. Therefore, neon seeding simulations were carried out, performing a seeding rate scan and an injected power scan while keeping the upstream electron density at the separatrix at 3×10^{19} m^{-3}. They show that at 15 MW of power injected into the edge plasma, the inner target is easily detached and presents low heat loads when neon is injected. However, at the outer target, the heat fluxes are not lowered below 10 MW/m^2, even when the power losses in the edge plasma are equal to 50% of the power crossing the separatrix. Therefore, the tokamak will probably need to be operated in a deep detached regime in its first phase of exploitation for discharges longer than a few seconds. In the framework of core–edge integrated modeling, using METIS, the power radiated in the core was computed for the most interesting cases.

KEYWORDS

JT-60SA, modeling, core, edge, scrape-off layer, power exhaust

1 Introduction

JT-60SA is an international fusion experiment built and operated by Japan and Europe, located in Naka, Japan. The JT-60SA tokamak is able to confine high-temperature deuterium plasmas lasting for a duration (typically 100 s) longer than the time scales characterizing key plasma processes, such as current diffusion and particle recycling, using superconducting toroidal and poloidal field coils [1]. During the initial research phase, the plasma-facing components (PFCs) of the tokamak will be entirely made of carbon tiles. The divertor will be *inertially cooled*. Under these conditions, the heat fluxes sustainable by the targets are estimated to be 10 MW/m^2 × 5 s, 3 MW/m^2 × 20 s, and 1 MW/m^2 × 100 s [1]. Therefore, at this stage, long plasma discharges will require very low-power fluxes at the targets. These conditions may be challenging to achieve, especially when operating the machine in the H-mode regime, where a narrow scrape-off-layer (SOL) decay length $\lambda_q \propto \frac{1}{B_p}$ is expected according to the existing multi-machine scaling [2].

In order to obtain low heat loads for longer discharges, the radiated fraction in the SOL has to be maximized through the injection of impurities, which can eventually lead to an advantageous condition where neutrals form a layer between the wall and the plasma, substantially reducing temperatures and heat loads on the plasma-facing components: this operational regime is called *detachment* [3–6]. However, impurities are transported through the main ion density gradient in the H-mode pedestal and can affect its stability by cooling down the core plasma and eventually leading to the loss of performances or even disruptions (see, for example, [7] and references therein).

When performing predictive modeling, the conflicting requirements of high core performance and efficient power exhaust demand simultaneous modeling of core and edge plasma. Within this framework, the aim of this paper is to simultaneously explore the core and divertor conditions for high-density unseeded and seeded scenarios, with mitigated heat fluxes and low core contamination from impurities for the initial phase of exploitation of the machine. The starting point for such a study has been the analysis of the already designed scenario 3 (see [1] for more details).

To do so, two codes have been interactively used: METIS, a fast global tokamak discharge simulator [8], and SOLEDGE3X–EIRENE in 2D transport mode, simulating the boundary plasma (i.e., edge and SOL) and the divertor region, with a treatment of plasma–wall interactions in a realistic (2D axisymmetric) wall geometry and a kinetic modeling of plasma-neutral interactions for atoms and molecules [9, 10].

The remainder of this paper is organized as follows: the integrated modeling strategy is presented in Section 2; the setup for simulations is discussed in Sections 3 and 4; Section 5 presents the main results of an unseeded density scan; and in Section 6 scenario 3 [1] is modeled, with both unseeded and seeded power scans and a neon seeding rate scan.

2 Core–edge integrated modeling: the method

In this section, the two codes SOLEDGE3X–EIRENE and METIS are described in brief, and the method for building complete scenarios from the interactive use of the two is presented.

2.1 Code descriptions and simulation domain

METIS is an integrated modeling tool that describes the plasma in 1D from the center up to the separatrix without providing an accurate description of plasma–wall interactions. Some of the most relevant outputs of METIS, providing an overall description of scenarios, are plasma equilibrium evolution and current diffusion, density and temperature profiles, and power loss profiles. On the other hand, SOLEDGE3X is a multi-species fluid code that can be run in two different ways: as a 2D mean-field transport code or as a 3D turbulent code. For kinetically modeling the transport of neutrals, SOLEDGE3X is coupled to the Monte Carlo code EIRENE [10]. Since it includes several atomic and molecular reactions [10], SOLEDGE3X–EIRENE models the edge and SOL regions with an accurate description of plasma–wall interactions in a realistic geometry (which makes it suitable for power-exhaust studies). However, extending the SOLEDGE3X–EIRENE domain deep into the core plasma would raise several modeling issues, due to the different physics of transport in core and edge plasma, and numerical issues, due to a possible increase in the time stepping. Therefore, the two codes have been interactively used complementarily, adopting the modeling strategy detailed in Section 2.2.

In this contribution, SOLEDGE3X–EIRENE is used in the 2D mean field transport mode, solving the particle, parallel momentum, and energy transport equations. The mesh grid covers a region of the plasma corresponding to the SOL and the outermost part of the confined region and is aligned with the magnetic flux surfaces. To deal with complex wall geometries, the grid is extended inside the wall, and a mask function determines which points are in the plasma and which points are in the wall. Wall boundary conditions are applied at the transition between the two sets of points [9]. In the vicinity of the strike points, the grid is aligned with the wall in order to improve the accuracy of the numerical discretization.

Using the code SOLEDGE3X–EIRENE in 2D mean-field mode means that radial transport is modeled as a diffusive process, with the equations of transport that are solved on a poloidal cross-section of the tokamak assumed to be toroidally symmetric. The SOLEDGE3X grid used is shown on the left side of Figure 1, and the EIRENE grid is shown on the right side of Figure 1.

For modeling the plasma core, METIS combines 0D scaling [11, 12]-normalized heat and particle transport, 1D current diffusion modeling, and 2D equilibria, allowing testing and optimizing time-dependent scenarios within a small computation time. The density and energy profiles are described on a 1D uniform grid on the normalized minor radius. The particle transport is not solved, and the electron density is defined through the prescription of some key parameters by the user: the line-averaged density ($\bar{n}_e$), the peaking factor $\frac{n_0}{n_e}$, the ratio between the central density and the volume average electron density, which is either prescribed or computed using a scaling expression, and the density value at the separatrix ($n_{e,a}$) obtained from simple models or scaling expressions [8]. The ion density is computed from Z_{eff}

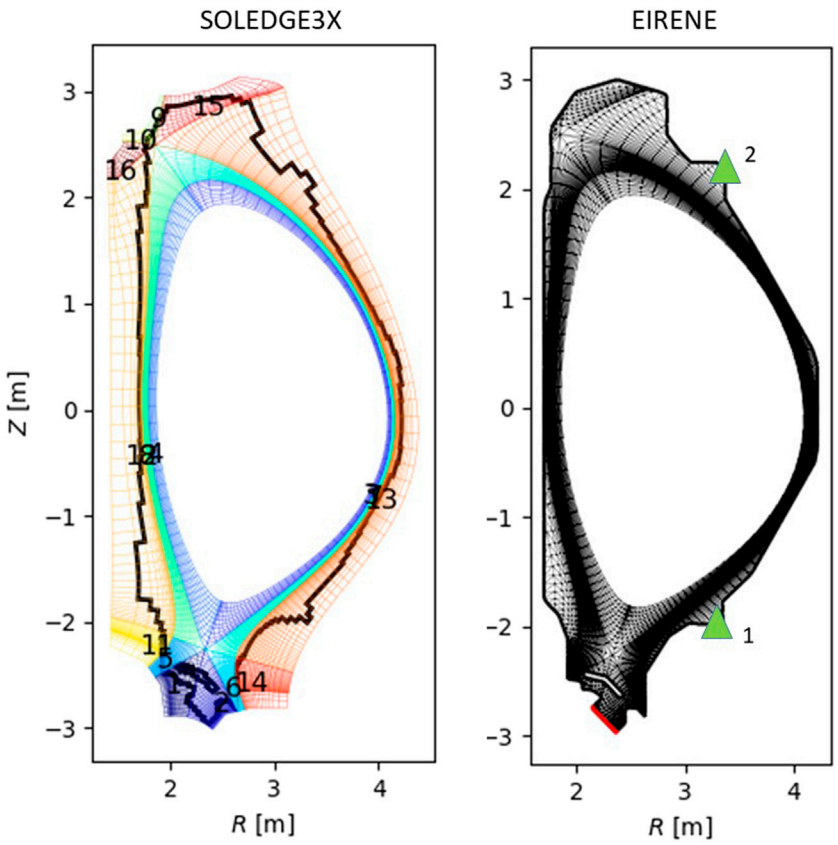

FIGURE 1
SOLEDGE3X and EIRENE grids. The latter shows puffs (green triangles) and pump (red) locations.

(effective charge) and the relative composition of the different species, both prescribed by the user. METIS is very well suited for scenario design due to the 1D radial and time-dependent input and output profiles and the computational throughput. An example of a JT-60SA scenario designed using METIS is shown in Figure 2.

2.2 Coupling SOLEDGE3X–EIRENE and METIS

In this work, the "coupling" of METIS and SOLEDGE3X–EIRENE means that the outputs of one code are used as inputs of the other and vice versa and does not refer to a real-time numerical coupling. Figures 1, 2 show that since one code is 1D and the other is 2D, a possible coupling is one-dimensional, with the 1D outer-midplane (OMP) profiles from SOLEDGE3X–EIRENE used as 1D inputs for METIS. The fact that the 2D profiles are neglected in favor of the OMP profiles when using the outputs from SOLEDGE3X–EIRENE as METIS inputs is one of the most significant approximations of our modeling strategy since the OMP profiles are not always representative of the 2D maps. However, we emphasize that while we point to a good description of the divertor conditions, we only aim at an estimation of the main core plasma parameters to obtain an overview of the impact of impurities on confined plasma, especially for highly seeded cases. Therefore, we believe that the approximations above are reasonable. In particular, we aim to check that the electron and ion temperatures are acceptable during seeding and estimate the power radiated in the core in order to compute the total power to inject into the plasma. The coupling procedure is described in the following paragraphs.

SOLEDGE3X–EIRENE has been employed to simulate various distinct physical conditions of the boundary region from the top pedestal to the wall, starting from certain values (inputs of the code) of particle flux (Γ) and power entering the edge domain (P_{edge}). For each case, energy sources and sinks, operational regimes, and heat loads at the targets have been studied.

Then, for few cases of interest, corresponding METIS simulations have been built, setting the inputs for METIS as the outputs of SOLEDGE3X–EIRENE cases at the OMP. The coupling point between the two codes has been set at the top pedestal, which for both codes is at $x \sim 0.95$.

In particular, the total injected power $P_{in,tot}$ has been chosen in METIS such that the difference between $P_{in,tot}$ and the integrated power radiated from the center of the plasma up to the top pedestal $P_{rad,core}$ is equal to P_{edge} (input of the corresponding SOLEDGE3X–EIRENE case) plus an extra power, called P_{ELMs}, and corresponding to a power accumulated in the pedestal

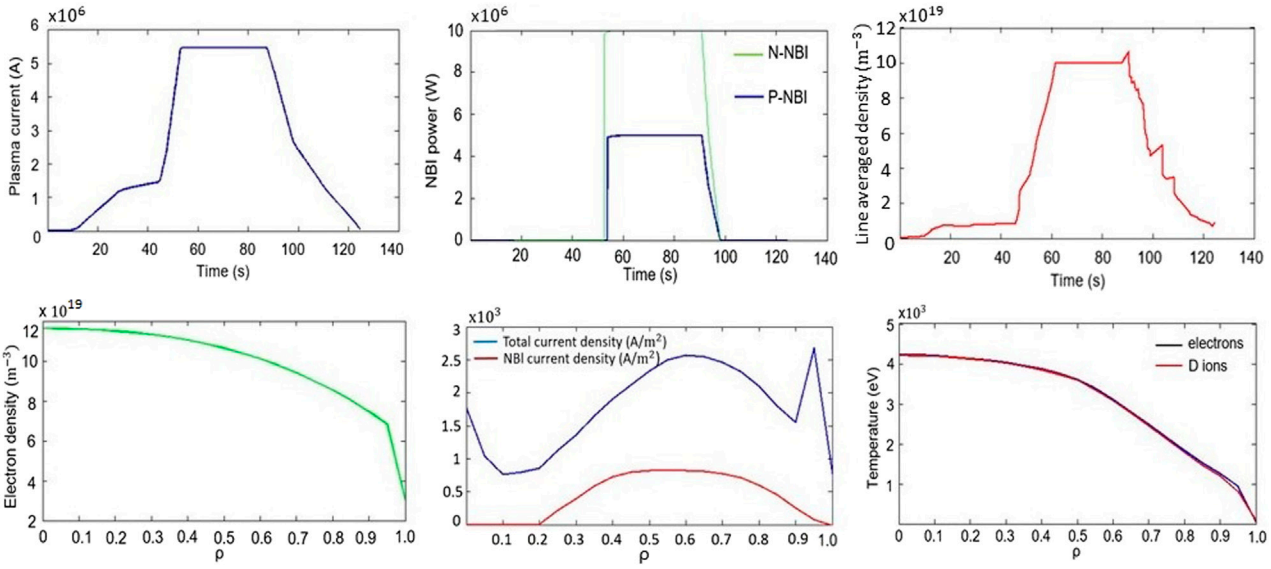

FIGURE 2
Example of some of the major quantities characterizing JT-60SA scenario 3 at half-power [1] in METIS. The 1D quantities on the second line are expressed in terms of the radial coordinate ρ and have been computed at t = 70 s (flat-top).

during the inter-ELM phase. The formula linking $P_{in,tot}$ (METIS input) and P_{edge} (SOLEDGE3X–EIRENE input) is then

$$P_{in,tot} = P_{edge} + P_{rad,core} + P_{ELMs}. \quad (1)$$

From the outputs of METIS and SOLEDGE3X–EIRENE cases, complete scenarios have been built, with an overview of most of the operational parameters.

The workflow is shown in Figure 3.

3 SOLEDGE3X–EIRENE simulation setup

SOLEDGE3X–EIRENE has been used in 2D mean-field mode without drifts. The simulations have been run with 10,000 particles per EIRENE stratum and a short cycling of 20, based on past sensitivity studies [13].

3.1 Fueling and heating

During the initial research phase, the neutral beam injection (NBI) will not be able to provide the full power of 34 MW foreseen for future tokamak operations; the positive NBI will provide at most 20 MW and the negative NBI will provide at most 10 MW, resulting in a total NBI power of 30 MW. Moreover, the electron cyclotron resonance frequency (ECRF) system will provide a maximum of 3 MW for a total heating power of 33 MW [1]. To take into account the power radiated in the edge and the ELM power (Eq. 1), the maximum power injected in the SOLEDGE3X-EIRENE domain has been equal to 20 MW. As boundary conditions, the deuterium particle influx from the core has been set to $S_D = 1.0 \times 10^{21}$ particles/s, accounting for NBI particle influx, and the carbon and neon influx to $S_C = S_{Ne} = 0$. The recycling coefficient R[1] has been set to 0.995 for the main plasma and neon ions on carbon tiles. For carbon ions on carbon tiles, the recycling coefficient has been set to R = 0.5, according to [14]. The particle influxes from the core and the recycling coefficient have been kept constant, and deuterium fueling has been used as the density control parameter. D_2 has been puffed from triangle 1, and neon from triangle 2, both shown in Figure 1 (right side). A source of carbon sputtered from the wall has been added to each case. The physical sputtering yield has been computed using the Bohdansky formula [15], and on top of it, a chemical sputtering with a constant rate has been added.

3.2 Assessment of the cross-field transport coefficients in the edge

The SOLEDGE3X–EIRENE code used in 2D transport mode emulates cross-field turbulent transport through effective *ad hoc* particle and energy diffusion [9], whose transport coefficients, $D_{\perp,eff}$ and $\chi_{\perp,eff}$ respectively, are usually chosen in agreement with experimental results. In order to reproduce the steep density and temperature profiles (*pedestal*) typical for H-mode regimes, the transport coefficients had to be set to vary as a function of the radial distance from the separatrix. In this work, since no experimental data were available, a heuristic approach has been used to determine the transport profiles based on the modification by using the two-point model [3] of transport profiles obtained from the modeling of existing

1 R is defined as the ratio between the recycled neutral flux and the outgoing ion flux.

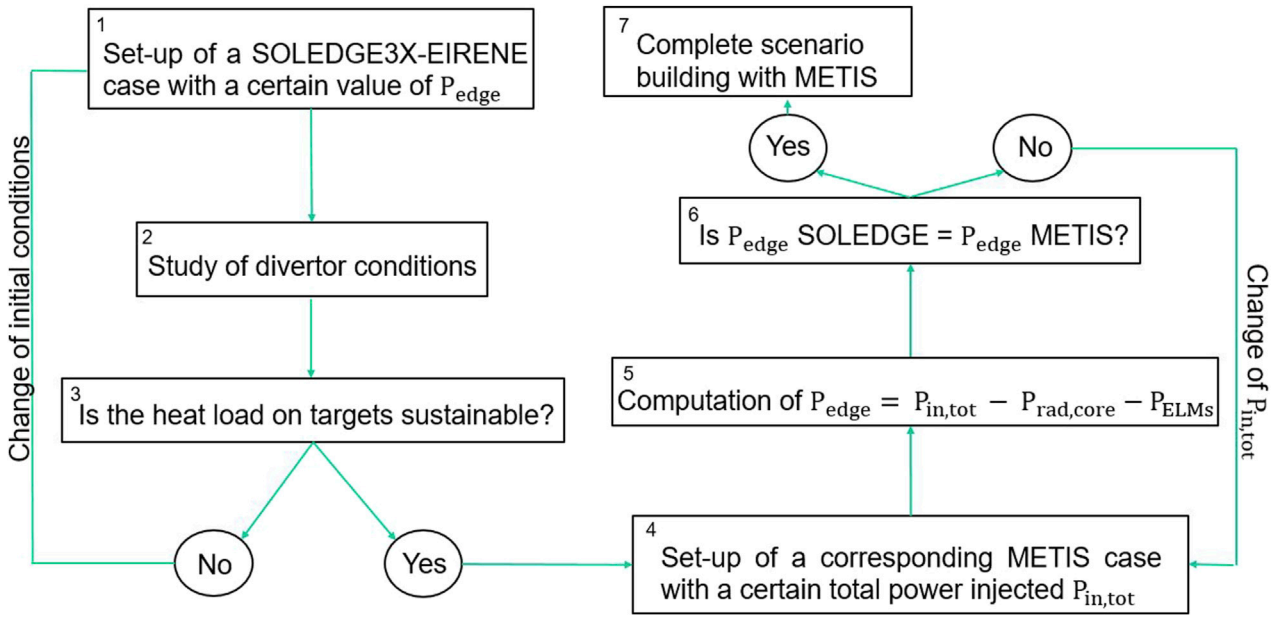

FIGURE 3
Integrated modeling work flow. The order of steps is given by increasing numbers.

machines. The method for choosing the diffusion coefficients has been detailed here. The diffusion profiles have been taken from [16], where they have been derived from the matching between JET simulations and data from JET discharges with parameters similar to our scenario of interest. However, since λ_q for JT-60SA is, in principle, different from the one for JET and the separatrix heat transport parameter $\chi_{\perp,eff\,sep}$ has a high influence on λ_q, $\chi_{\perp,eff\,sep}$ has been modified to a value compatible with the JT-60SA parameters. In order to do that, Formula 2 has been used, derived in [3] assuming an exponential decay of the heat flux in the SOL and a dependence of the upstream density on the upstream temperature as given by the two-point model for high-recycling and detached regimes:

$$\chi_{\perp,eff\,sep} = \frac{1}{n_{e,u}}\left(\frac{k_0^2 N^4 P_{SOL}^5}{R^9 a^5 k^5 q_{95}^4}\right)^{\frac{1}{7}} \lambda_q^{\frac{9}{7}}, \quad (2)$$

where $N = 1$ is the number of nulls in the poloidal field, $n_{e,u}$ is the upstream (i.e., where the OMP intersects the separatrix) electron density, P_{SOL} is the power crossing the separatrix, R and a are the major and minor radii, respectively, k is the elongation, and k_0 is the conduction coefficient of the Spitzer–Harm equation:

$$k_0 = \frac{(4\pi\epsilon_0)^2}{m_e^{1/2} ln\Lambda e^4 Z},$$

and λ_q is the SOL width decay length [2]. It has been computed from the Eich scaling law [2]:

$$\lambda_q = C_0 B_T^{C_B} q_{cyl}^{C_q} P_{SOL}^{C_P} R_0^{C_R}, \quad (3)$$

with coefficients C_0, C_B, C_q, C_P, and C_R taken from Table 1.

TABLE 1 Estimators for the coefficients in the Eich scaling law with their respective variances. Values taken from [2].

C_0	C_B	C_q	C_P	C_R
0.73 ± 0.38	−0.78 ± 0.25	1.20 ± 0.27	0.10 ± 0.11	0.02 ± 0.20

The value obtained for λ_q is equal to 1.4 mm, lower with respect to already working machines (e.g., JET and ASDEX [2]) and in agreement with the predictions of $\lambda_q \sim 1$ mm for ITER [2]. The value of 1.4 mm for λ_q is probably an underestimate for high-density cases like the ones studied in this work. A broadening of λ_q by a factor of up to 4 with respect to the value obtained by the Eich scaling (Eq. 3) is foreseen in high-density cases [17]. Supplementary Appendix S2 provides a validation of the transport profiles, showing that the method adopted for setting up the transport profiles returns in simulations in attached conditions the value of λ_q expected by the Eich scaling.

The $D_{\perp,eff}$ profile has not been changed with respect to the profile from tuning on JET data. The same heat and particle diffusion coefficient profiles have been set for electrons, main ions, and impurities. The diffusion profiles derived from the aforementioned model for a case with P_{edge} = 15 MW and $n_{e,u}$ = 3×10^{19} m^{-3} are given in Figure 4. We have applied such transport coefficients to all the cases simulated.

4 METIS simulation setup

In this work, METIS simulations have been run for scenario 3, whose main free parameters are given in Table 2. However, METIS

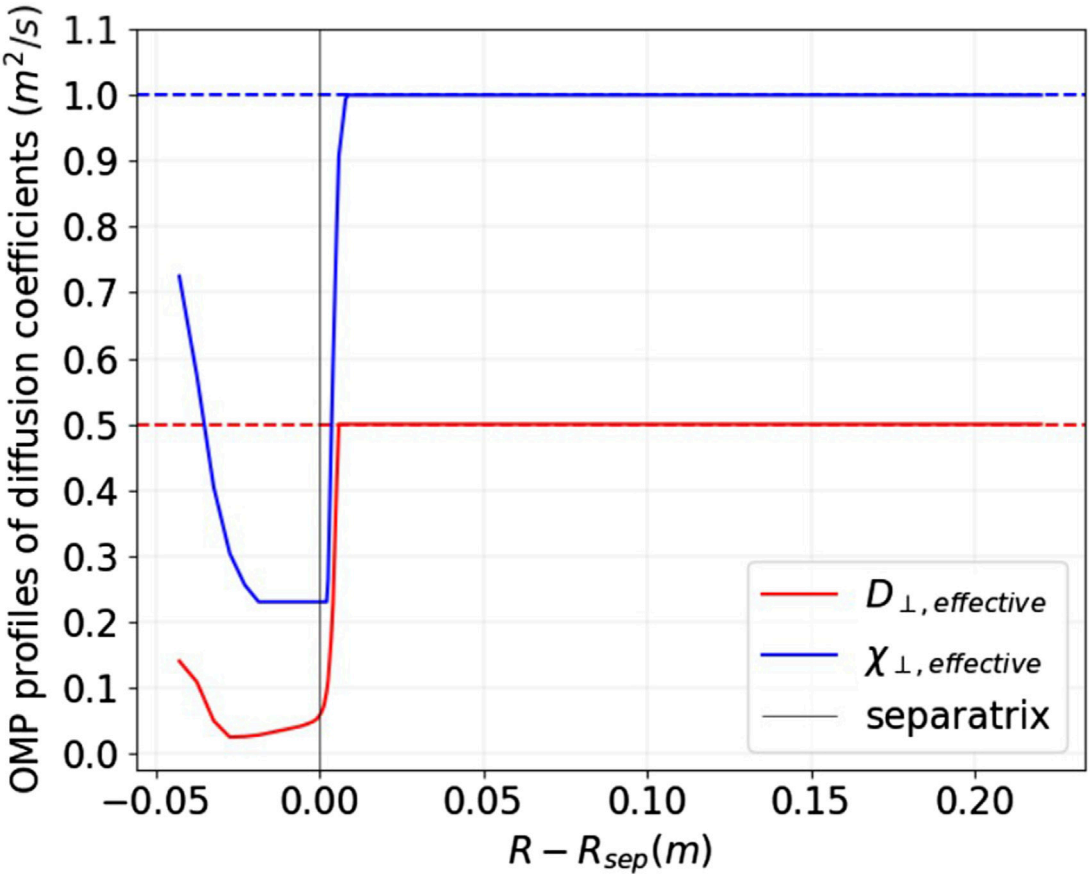

FIGURE 4
Diffusion coefficient profiles (in solid lines) at the OMP used for the scenario proposed at P_{edge} = 15 MW and $n_{e,u} = 3 \times 10^{19}$ m^{-3}. $\chi_{\perp,eff}$ is the same for all ion species and electrons, and $D_{\perp,eff}$ is the same for all ion species. Poloidal symmetry is assumed.

TABLE 2 Main parameters of scenario 3 foreseen for the JT-60SA tokamak.

I_P (MA)	B_T (T)	N-NBI, P-NBI, and ECRH power (MW)	$\bar{n}_e$ (line average) (10^{20} m^{-3})
5.5	2.25	10, 20, and 0	1.0

requires setting up some extra free parameters, which have been chosen here as explained below.

For a good estimation of the power radiated in the core, the most important free parameters to be set in METIS are Z_{eff}, the density at the separatrix $n_{e,a}$, the density peaking factor, and the density at the pedestal. $n_{e,a}$ has been set equal to 3×10^{19} m^{-3}, which is ~ 1/3 of the foreseen line averaged density [1] (Table 2), and the same value is imposed in SOLEDGE3X–EIRENE for scenario 3. The peaking factor has been tuned in order to obtain an H-mode profile with central density and density at the separatrix as prescribed by [1] (see the profile in Figure 2) and pedestal density equal to the one obtained from the corresponding SOLEDGE3X–EIRENE simulations.

Z_{eff} is a crucial parameter that needs to be prescribed for computing the power radiated with METIS since the density of the major impurity is determined by the code combining the quasi-neutrality condition with its definition $Z_{eff} = \frac{\sum_i n_i Z_i^2}{\sum_i n_i Z_i}$, where n_i is the density of a charged ion state i, Z_i is its charge, and n_e is the density of electrons. The density of deuterium and the density of the most abundant impurity are the unknowns in the system; if more than one impurity is present, the densities of the other impurities are computed as a percentage (to be prescribed by the user) of the density of the most abundant one. All the densities are dependent on the radial coordinate x and time t, but Z_{eff} is constant along x.

In order to be coherent with the SOLEDGE3X–EIRENE simulations, the constant value of Z_{eff} to be set up in METIS has been chosen as the value of the same OMP quantity at the separatrix, given as output by SOLEDGE3X–EIRENE; the values obtained for neon-seeded cases are shown in the central plot of Figure 12. The same has been done for prescribing the ratio between impurities in neon-seeded cases.

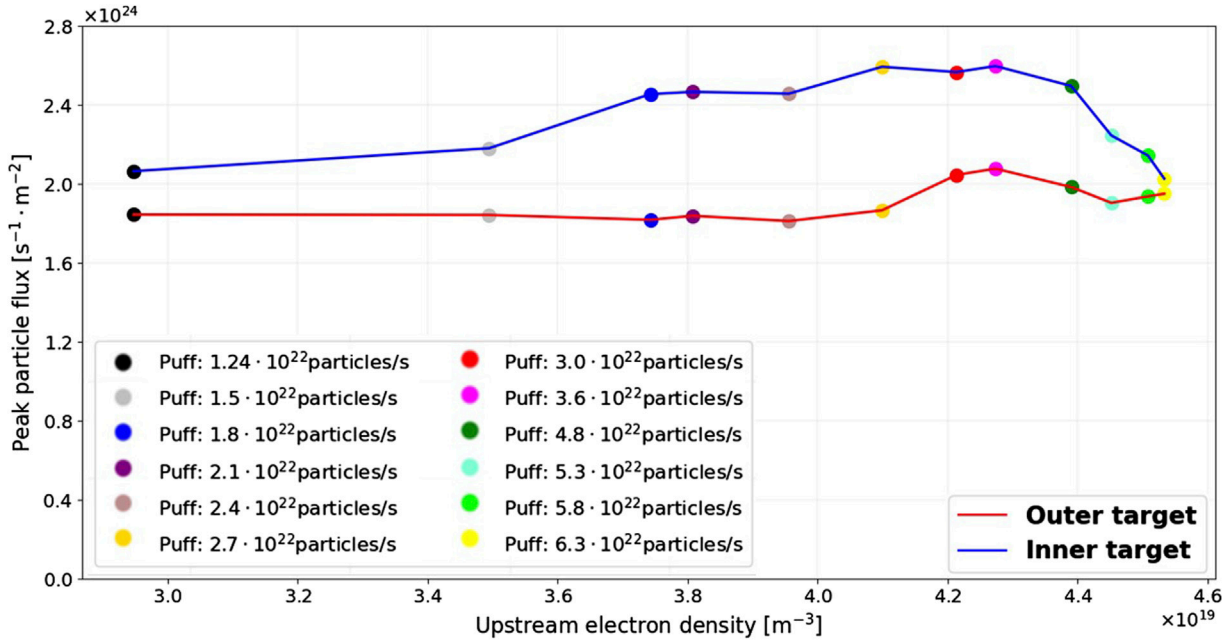

FIGURE 5
Peak particle flux at the targets as a function of the upstream electron density for a deuterium puff rate scan. Each point represents a different simulation with a different puff rate.

5 Unseeded cases: density scan

As a preliminary analysis, a density scan without impurity injection has been carried out with the purpose of studying how to reach detachment in unseeded cases. The throughput (i.e., D_2 puff) has been increased at a fixed edge power P_{edge} = 15 MW. In Figure 5, the peak particle influx at the inner and outer targets as a function of the upstream electron density is plotted. At the inner target, an increase in the particle flux can be observed from 3 to 4.2 × 10^{19} m^{-3}; beyond that value, the particle flux starts decreasing with the typical roll-over, meaning that the plasma starts to detach from that point on. This is confirmed by the flat electron temperature profile at 1 eV for the highest density cases (Figure 7, bottom) and by the fact that the ionization front is detached from the strike point and recombination takes place at the target, as shown in Figure 6. The first point of the scan ($n_{e,u} = 3 \times 10^{19}$ m^{-3}) is already in a high-recycling regime since the particle flux grows more slowly than the $\propto n_u^2$ dependence typical of conduction-limited regimes [3]. The outer target presents a flat peak particle flux profile without a clear roll-over, with electron temperatures at approximately 5 eV and the ionization front still attached to the target for the highest density case (Figure 6). On the other hand, although the peak heat loads (Figure 7, top) of the highest density case are lower than 10 MW/m^2, they are still significant.

The whole picture described in this section seems to suggest that, under these conditions, the density will need to be increased further to obtain full detachment at the outer target and/or heat fluxes sustainable for more than a few seconds. An alternative to the increase in density is to inject impurities into the SOL or to operate at low power.

6 Scenario 3 modeling

We are mainly interested in investigating the heat fluxes for the scenarios designed in the Research Plan 2018. Being the scenario with the foreseen highest line-averaged density ($\bar{n}_e = 10^{20}$ m^{-3} = 0.8 $n_{Greenwald}$), the scenario 3 is most promising in terms of power exhaust among the ones proposed by the Research Plan 2018 [1]; because of that, it has been simulated and analyzed in this work as a starting point for power and seeding rate scans to explore the operational parameters eventually leading to mitigated heat fluxes at the targets. Its main parameters are shown in Table 2.

From the L → H transition scaling law, $P_{LH} = 1.38\,(\bar{n}_e/10^{20})^{0.77} B^{0.92} R^{1.23} a^{0.76}$ MW [18] the lowest value of net power guaranteeing H-mode regime operation has been found to be 12.5 MW.

6.1 Unseeded cases

From Eq. 1, the power to be given to SOLEDGE3X–EIRENE is the net power minus P_{ELMs} minus the power radiated in the core. Therefore, assuming zero radiation in the core, we will obtain the highest limit for the minimum power to set up in SOLEDGE3X–EIRENE to be in H-mode: $P_{edge\ min} = P_{LH} - P_{ELMs}$. P_{ELMs} has been estimated to be (5.0 ± 0.5) MW based on the study of the diamagnetic energy variation in the JET shot number 92141 carried out in [19]. Since it is proportional to the ELM frequency, which is proportional to the heating power [20], P_{ELMs} is likely a function of the injected power. However, a detailed analysis of ELMs in a JT-60SA highly radiative scenario is out of the scope of the present work, and the estimation of

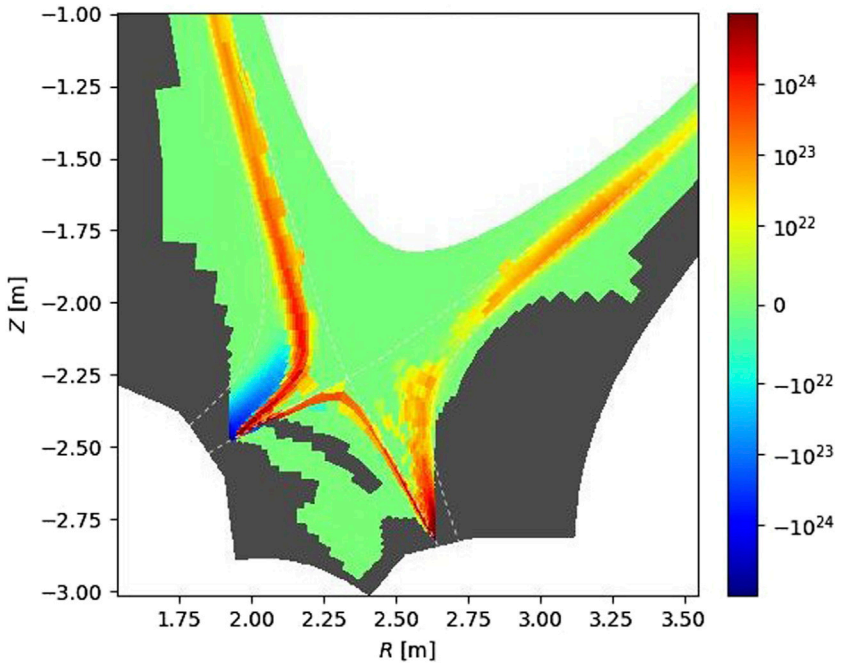

FIGURE 6
Source of neutral deuterium close to the targets for the case at the highest density ($n_{e,u} = 4.5 \times 10^{19}$ m^{-3}) in the puff rate scan of Figure 5. The color bar has been set on a logarithmic scale, where negative source values correspond to recombination dominating and positive source values to ionization dominating.

P_{ELMs} = (5.0 ± 0.5) MW will be applied regardless of the injected power. Therefore, $P_{edge\ min}$ = (12.5 − 5.0) MW = 7.5 MW.

The puff of D_2 has been tuned in order to obtain an upstream electron density equal to $n_{e,u} = 3 \times 10^{19}$ m^{-3} (~1/3 of $\bar{n}_e$) [1], and a power scan has been carried out without impurity injection, with the resulting heat loads and temperature at the targets shown at the top and bottom of Figure 8, respectively.

The only case to be sustainable for the targets is the case at low power P_{edge} = 10 MW. Therefore, the heat loads at the targets for higher-injected power cases need to be lowered through impurity injection.

6.2 Neon-seeded cases

Two different scans have been carried out when including neon seeding: a neon injection rate scan at fixed P_{edge} and a power scan at a fixed neon injection rate.

For the former, the deuterium puff rate has been fixed to 2.4×10^{22} particles/s and the power to P_{edge} = 15 MW, varying the neon injection rate from 3×10^{20} particles/s to 12×10^{20} particles/s. Under such conditions, the OMP electron density at the separatrix is between 2.8 and 3.0×10^{19} m^{-3}. For the latter, the neon puff has been set to 3×10^{20} particles/s, and P_{edge} has been increased up to 17 and 20 MW. The heat loads and temperatures at the targets resulting from the neon injection rate scan are shown in Figure 9, and those from the power scan are shown in Figure 10. The injection of neon causes the growth of the asymmetry between the heat loads on the inner and outer targets, as observed when comparing Figure 8 and Figure 10. This could be due to the higher concentration of impurities at the inner targets with respect to the outer target for seeded cases, at the opposite of what happens for unseeded cases, as shown in Figure 11. We point out that carbon, which at first is sputtered mainly from the outer target because of the higher temperatures (Figure 11, left), globally decreases when neon is puffed (the total carbon content decreases from 3×10^{19} to 0.5×10^{19} carbon particles after neon injection). Additionally, as observed from the difference in carbon density at the targets between the left and the central plot of Figure 11, carbon migrates toward the inner target when adding seeding. Furthermore, a higher neon density is observed at the inner target with respect to the outer target. The higher impurity fluxes at the inner target are mainly due to friction forces, both for carbon and neon.

Figure 9 (bottom) shows an increase in the electron temperature at the outer target with increasing neon puff. However, the heat fluxes decrease (Figure 9, bottom) due to a simultaneous decrease in electron density.

The effects of increasing neon puff on the edge plasma can be mainly studied through the computation of the total power radiated in the SOL, as shown in Figure 12 (left), while the core contamination is taken into account by Z_{eff} at the separatrix, whose value is given in Figure 12 (right), and by the estimation of the power radiated in the core computed using METIS, which is shown in Table 3. It can be observed that most of the core radiation is from bremsstrahlung, mainly generated by fully or partially ionized carbon and neon particles entering the core. METIS simulations without neon injection show that the power radiated in the core is approximately 2 MW (when P_{edge} =

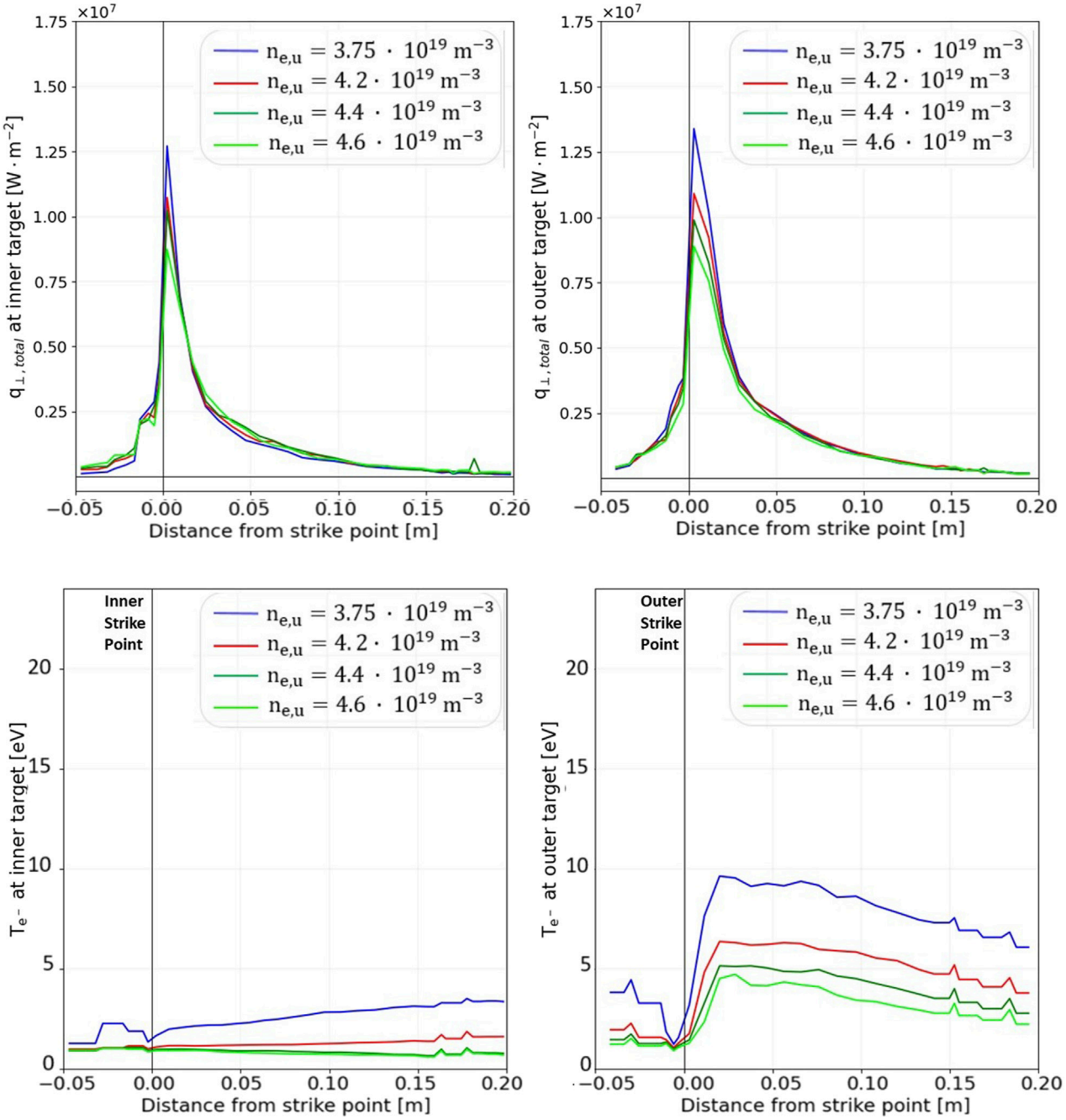

FIGURE 7
Total (ions, neutrals, and radiation) perpendicular heat flux (top) and electron temperature (bottom) at the inner and outer targets as a function of the distance from the respective strike points for a sub-set of the deuterium puff scan in Figure 5.

15 MW), even for unseeded cases, mainly due to ionized carbon in the core. On the other hand, the power radiated by line radiation is low for unseeded cases and low-neon puff cases, as expected, since carbon is fully ionized at temperatures lower than the typical core temperatures of such machines. The electron and ion temperatures in the core do not decrease significantly during high seeding, in the limit of the light coupling performed in this work between SOLEDGE3X–EIRENE and METIS.

One can see that for all the neon-seeded cases, the temperature at the strike points is very low and compatible with a safe operation. On the contrary, the peak heat flux at the outer target is slightly above 10 MW/m^2, which could imply a limitation in the discharge duration. Because of that, the machine will probably need to be operated in deep detached regimes in its first phase of exploitation. This is even truer when considering that all the simulations presented did not include drifts; it is probable that the drift terms would further move the operational space in the direction where relatively deep detachment is necessary, as they might increase the

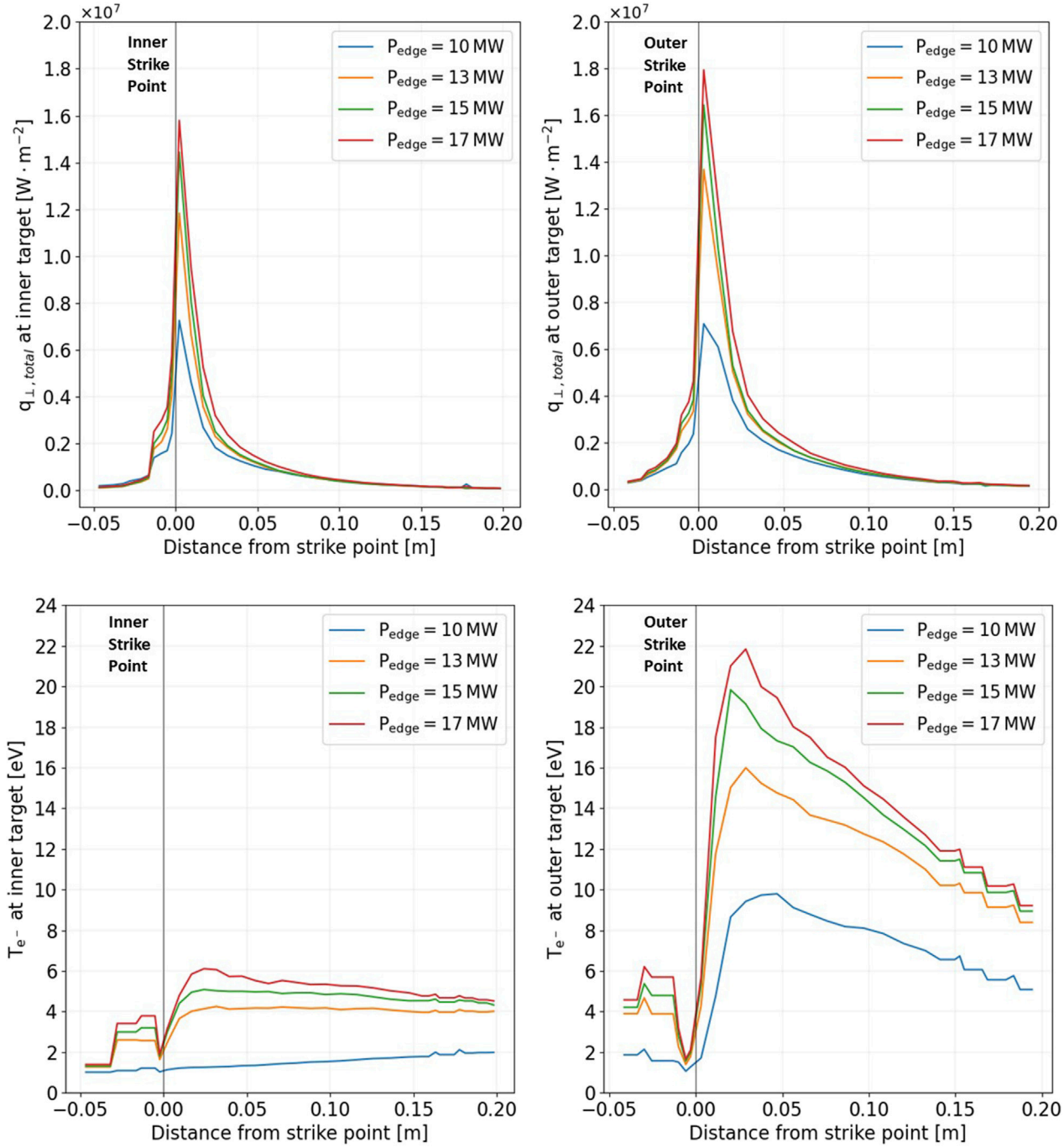

FIGURE 8
Total (ions, neutrals, and radiation) perpendicular heat flux (top) and electron temperature (bottom) at the inner and outer targets as a function of the distance from the respective strike points for an unseeded power scan at P_{edge} = 10, 13, 15, and 17 MW.

asymmetry between inner and outer targets in favor of higher heat fluxes at the outer target.

However, further studies on the sensitivity of such a peak heat flux with respect to the cross-field transport coefficients will be needed to verify whether a less conservative assumption, i.e., a larger value on the $\chi_\perp$ parameter, according to what has been found in present experiments for high-density and high recycling conditions, will reduce such a peak to acceptable values for discharges lasting longer than few seconds.

6.3 Higher-deuterium puff scenarios with neon seeding

Starting from the simulations presented above, an attempt to scan for higher deuterium and/or higher neon injection rates has been carried out. In such high particle injection cases, SOLEDGE3X–EIRENE simulations reach a state where deuterium highly recombines at the divertor, leading to high neutral pressure and a subsequent increase in the main plasma

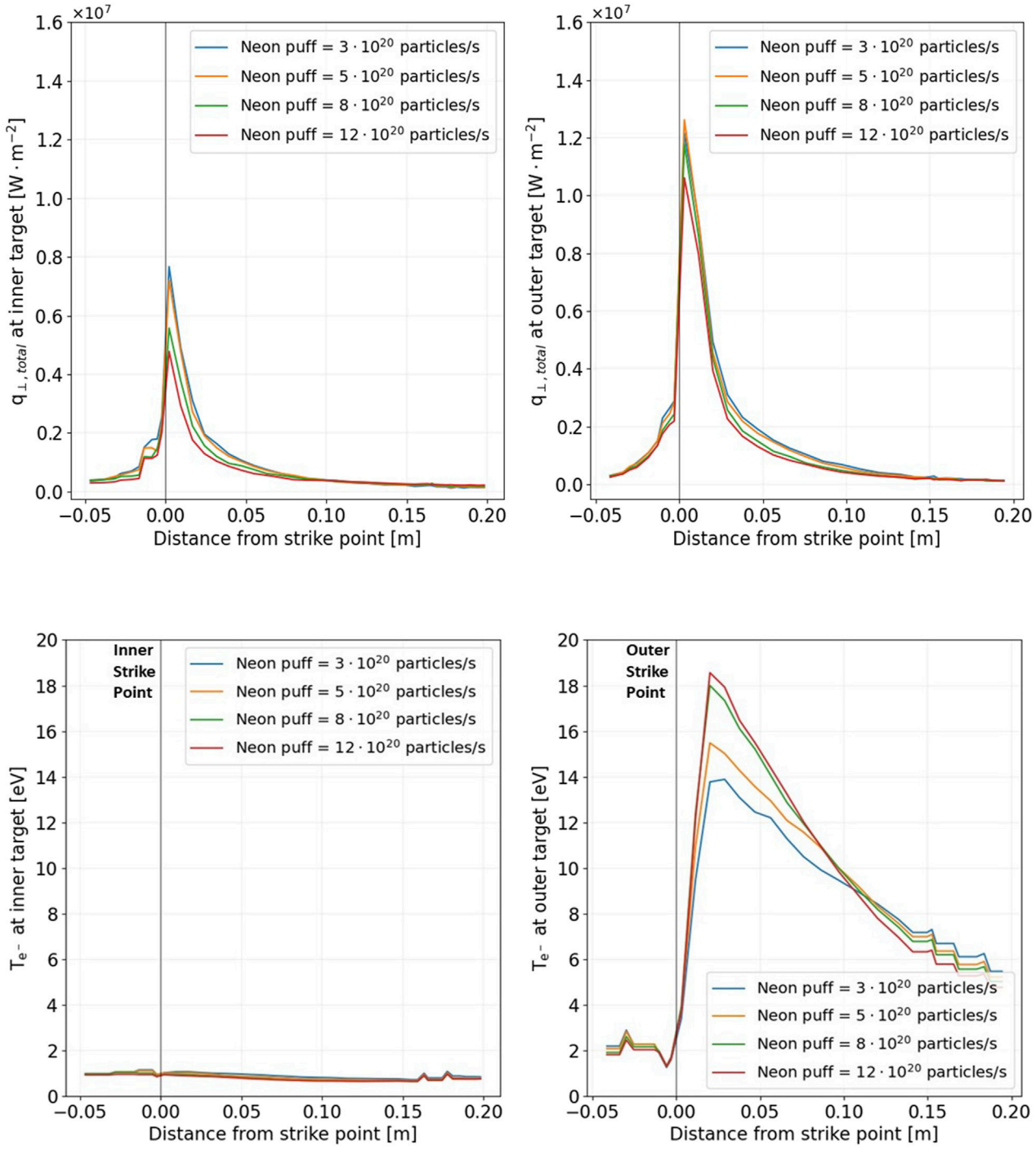

FIGURE 9
Total (ions, neutrals, and radiation) perpendicular heat flux (top) and electron temperature (bottom) at the inner and outer targets as a function of the distance from the respective strike points for a neon seeding rate scan at P_{edge} = 15 MW. Deuterium puff = 2.4 × 10^{22} particles/s.

out-flux, especially at the inner target. This mechanism is responsible for a long computational time, which is the reason why such simulations have not reached a steady state yet.

The source of neutrals at the targets in an example case for such a high recombination state (deuterium puff equal to 3 × 10^{22} particles/s and neon puff to 15 × 10^{20} particles/s) and the source of neutrals for a converged case with slightly lower particle injection (deuterium puff equal to 2.4 × 10^{22} particles/s and neon puff to 8 × 10^{20} particles/s) can be compared when analyzing Figure 13. The same picture on the right-hand side of Figure 13 is found when puffing deuterium at a rate of 4 × 10^{22} particles/s and neon at a rate of 10 × 10^{20} particles/s.

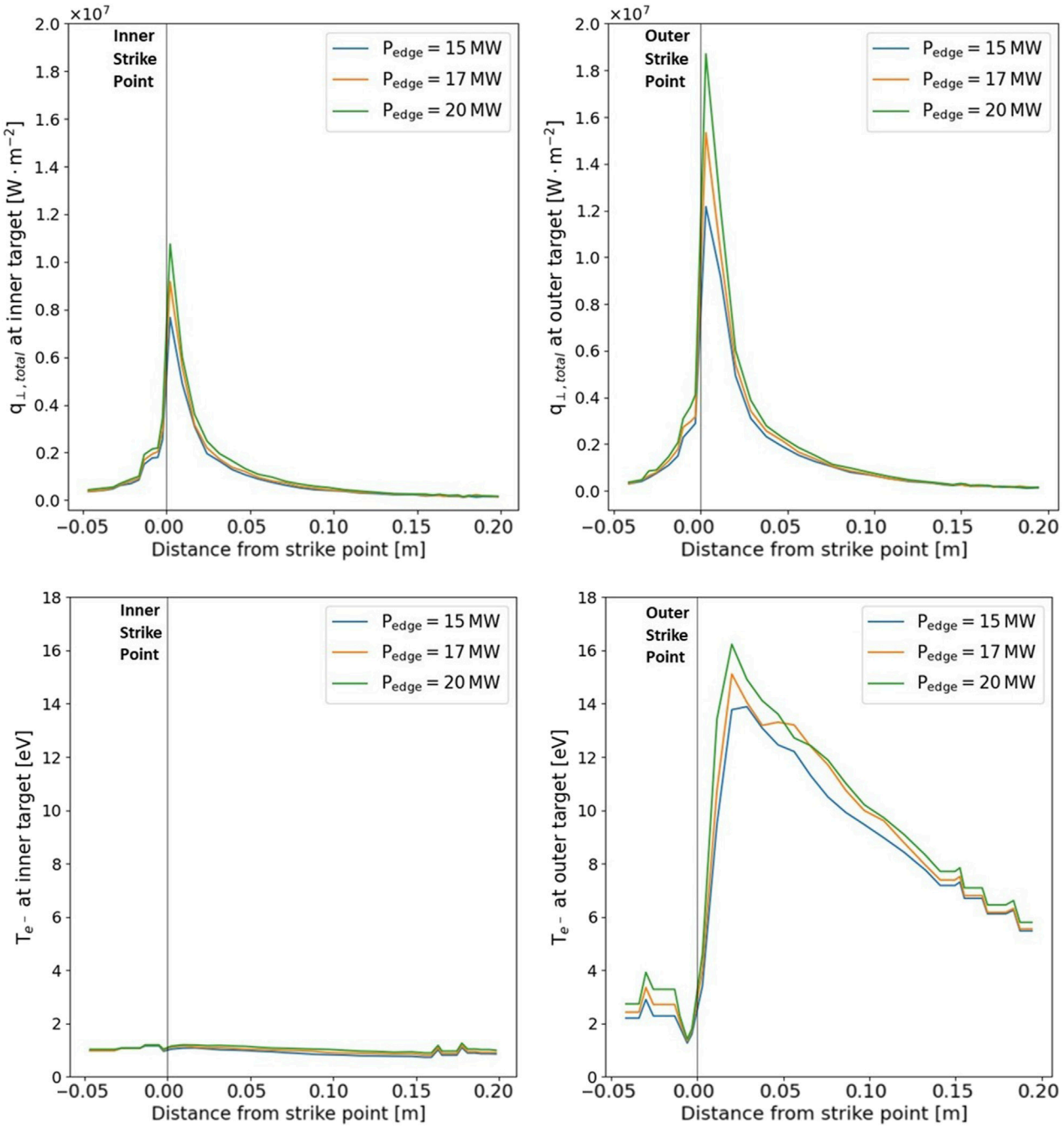

FIGURE 10
Total (ions, neutrals, and radiation) perpendicular heat flux (top) and electron temperature (bottom) at the inner and outer targets as a function of the distance from the separatrix for a neon-seeded (injection rate = 3×10^{20} particles/s) power scan at P_{edge} = 15, 17, and 20 MW.

7 Conclusion

This contribution aimed to investigate the operational conditions needed to carry out long pulses during the initial research phase of the JT-60SA tokamak with a carbon wall and inertially cooled divertor.

Starting from scenario 3 designed in the Research Plan 2018, highly radiative H-mode scenarios have been explored through the integrated use of the codes SOLEDGE3X-EIRENE (in 2D configuration) and METIS, with the aim of identifying the physical conditions needed to run the tokamak with heat fluxes at the targets significantly lower than 10 MW/m^2, and potentially operating the divertor in a detachment regime while maintaining high-core plasma performances.

A first analysis has focused on unseeded cases: the conditions for early detachment in unseeded shots have been investigated, showing

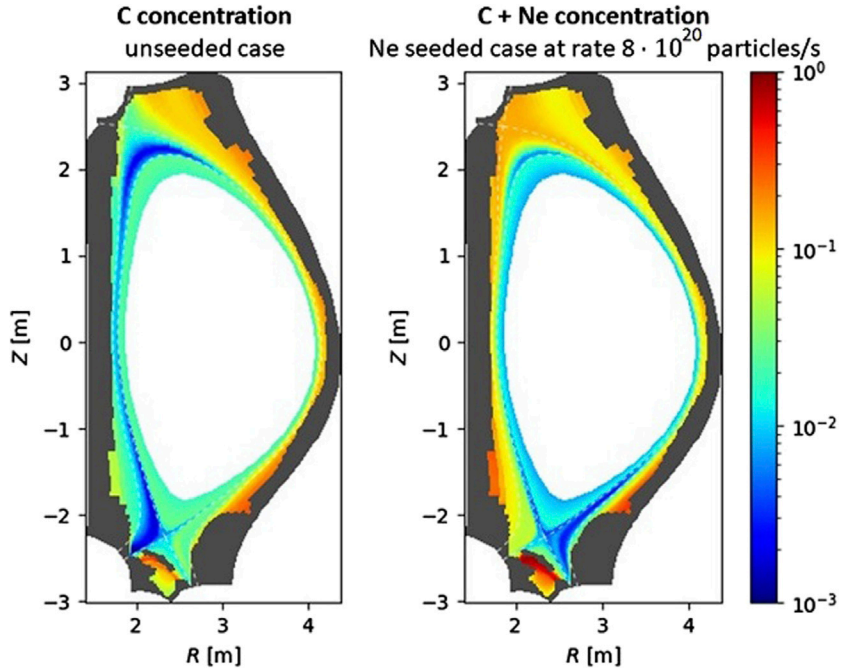

FIGURE 11
2D plot of impurity concentration for the unseeded case with P_{edge} = 15 MW (left side) and for a seeded case with neon injection at a rate of 8×10^{20} particles/s (right side). The color map has been set on a logarithmic scale.

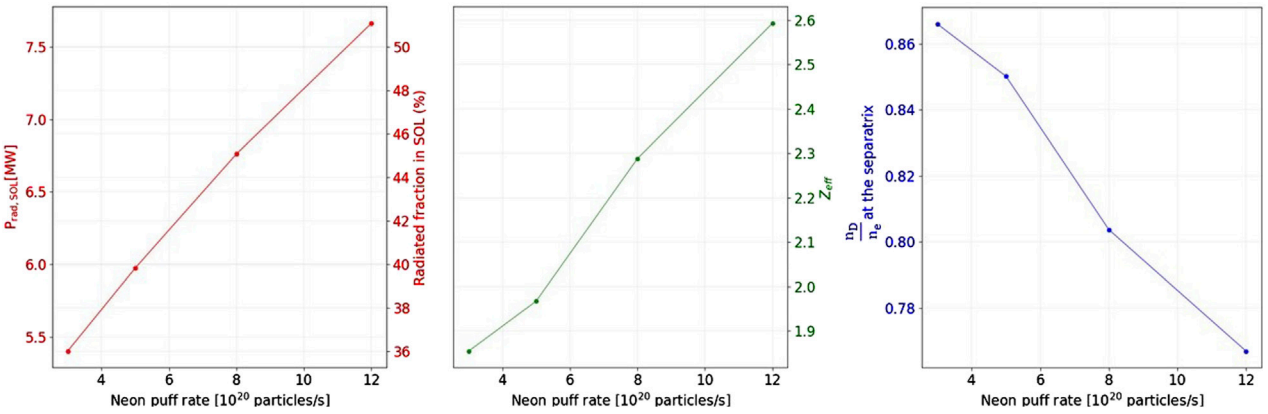

FIGURE 12
Total power radiated in the SOL (left side), values of Z_{eff} at the separatrix (central plot), and values of plasma purity (relative concentration of deuterium) at the separatrix (right side) for a neon seeding scan.

TABLE 3 Computation of $P_{rad,core}$ for neon puff scan cases, starting from P_{edge} = 15 MW. The power radiated in the core has been computed using METIS as the sum of the power emitted through line radiation $P_{lineRad}$ and bremsstrahlung P_{brem}.

Ne puff (10^{20} particles/s)	$P_{in,tot}$ (MW)	P_{ELMs} (MW)	$P_{rad,core}$ (P_{brem} + $P_{lineRad}$) (MW)
3.0	22.8	5	2.3 + 0.5
5.0	23.1	5	2.4 + 0.7
8.0	23.8	5	2.9 + 0.9
12.0	24.5	5	3.4 + 1.1

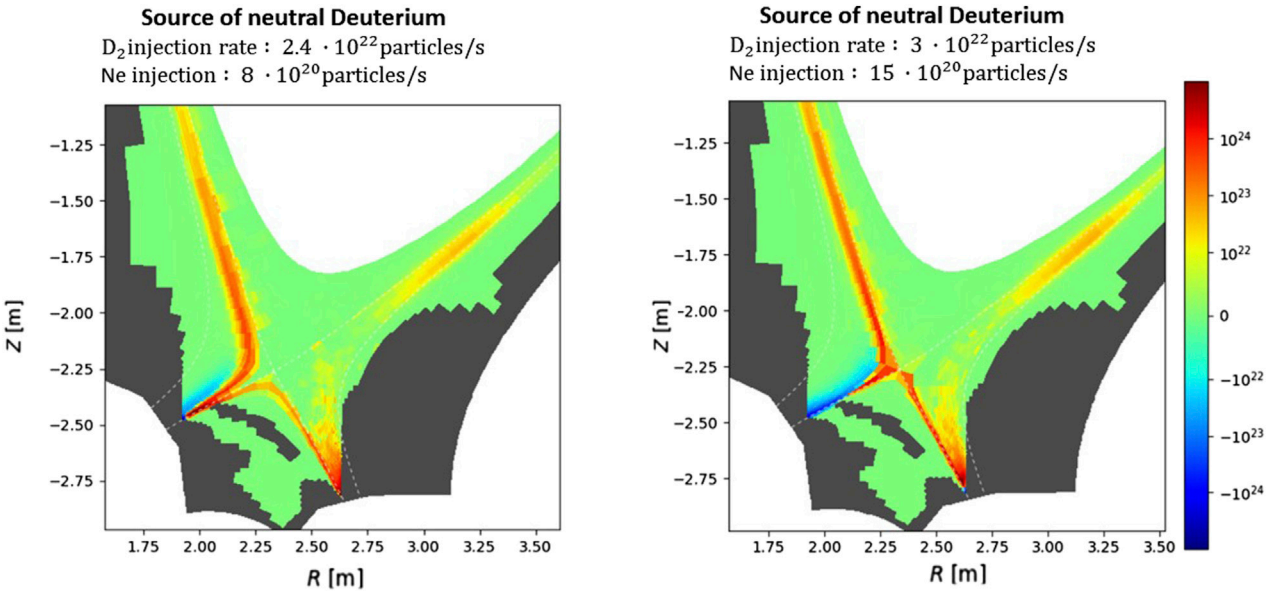

FIGURE 13
Source of neutral deuterium close to the targets for a steady-state case (left-hand side) and a case with higher deuterium and neon injection (right-hand side). The latter case has not reached a steady-state yet. The color bar has been set on a symmetric logarithmic scale, where a negative source value corresponds to recombining plasma (recombination-dominating ionization).

that an upstream electron density higher than 4.2×10^{19} m^{-3} is required, with heat loads close to the operational limit of 10 MW/m^2 even in the highest density case analyzed. This shows that achieving low heat loads without impurity seeding will probably be challenging for JT-60SA in its first phase of exploitation and will require very high densities. However, the cases with the highest density among the ones simulated show electron temperatures lower than 5 eV on both targets.

Neon-seeded cases have been investigated through power and impurity concentration scans, where strong asymmetry between the outer and inner targets has been observed in all cases.

It has been shown that obtaining low heat fluxes at the outer target is particularly challenging, even for highly seeded, high-density plasmas. As proof for this statement, we show a case with a total injected power of 24.5 MW. It has an upstream electron density between 2.8×10^{19} m^{-3} and 3×10^{19} m^{-3}; ~18% of the total power is radiated in the core, and ~50% of the power entering the edge is radiated in the SOL. While showing low heat fluxes at the inner targets (below 5 MW/m^2), it presents perpendicular heat loads at the outer target close to 10 MW/m^2, which could prevent safe operation for discharges lasting longer than few seconds. This points toward the need to operate the machine in deep detachment with very high-power radiated fractions during its initial phase of exploitation. The power radiated in the core has been computed using METIS for computing the total injected power. When analyzing core conditions, in the limit of the light coupling performed in this work, there is no signal for decreasing core performances since the ion and electron temperatures do not decrease in the highest seeding cases simulated here.

Lower heat fluxes could be obtained by relaxing the assumption of a small SOL width (λ_q ~ 1.4 mm), according to the broadening of the SOL width foreseen for high-density plasmas [17].

An attempt to simulate fully detached cases in the framework of scenario 3 has been carried out through a neon high-rate injection. In such cases, it has been observed that the fast decrease in temperature leads to massive deuterium recombination. Since we did not manage to run them to a steady state, we refer to a future publication for an analysis of their results.

Data availability statement

The original contributions presented in the study are included in the article/Supplementary Material; further inquiries can be directed to the corresponding author.

Author contributions

LG: conceptualization, data curation, investigation, software, writing–original draft, and writing–review and editing. GC: project administration, supervision, and writing–review and editing. GG: project administration, supervision, validation, and writing–review and editing. GF: conceptualization, methodology, validation, and writing–review and editing. NR: investigation, software, supervision, validation, and writing–review and editing. KG: conceptualization, investigation, methodology, supervision, and writing–review and editing. LB: conceptualization, methodology, and writing–review and editing. NV: data curation, investigation, software, and writing–review and editing. SS: data curation, investigation, software, and writing–review and editing. JA: software and writing–review and editing. HB: software and writing–review and editing. RD: software

and writing–review and editing. AG: methodology and writing–review and editing. PG: methodology and writing–review and editing. VQ: software and writing–review and editing. GR: methodology and writing–review and editing. PT: formal analysis, software, validation, and writing–review and editing.

Funding

The author(s) declare that financial support was received for the research, authorship, and/or publication of this article. This work was carried out within the framework of the EUROfusion Consortium, funded by the European Union via the Euratom Research and Training Programme (grant agreement no. 101052200 EUROfusion) and the European Union's Horizon 2020 research and innovation program under grant agreement no. 824158 (EoCoE-II).

Conflict of interest

The authors declare that the research was conducted in the absence of any commercial or financial relationships that could be construed as a potential conflict of interest.

Publisher's note

Author disclaimer

Views and opinions expressed are those of the author(s) only and do not necessarily reflect those of the European Union or the European Commission. Neither the European Union nor the European Commission can be held responsible for them.

Supplementary material

The Supplementary Material for this article can be found online at: https://www.frontiersin.org/articles/10.3389/fphy.2024.1422286/full#supplementary-material

References

1. JT-60SA. Jt – 60sa research plan: research objectives and strategy. (2018). Available from: http://jt60sa.org/pdfs/JT–60SAResPlan.pdf.

2. Eich T, Sieglin B, Scarabosio A, Fundamenski W, Goldston RJ, Herrmann A, et al. Inter-elm power decay length for jet and asdex upgrade: measurement and comparison with heuristic drift-based model. *Phys Rev Lett* (2011) 107:215001. doi:10.1103/physrevlett.107.215001

3. Pitcher CS, Stangeby P. Experimental divertor physics. *Plasma Phys Controlled Fusion* (1997) 39:779–930. doi:10.1088/0741-3335/39/6/001

4. Leonard AW. Plasma detachment in divertor tokamaks. *Plasma Phys Controlled Fusion* (2018) 60:044001. doi:10.1088/1361-6587/aaa7a9

5. Loarte A, Monk R, Martín-Solís J, Campbell D, Chankin A, Clement S, et al. Plasma detachment in jet mark i divertor experiments. *Nucl Fusion* (1998) 38:331–71. doi:10.1088/0029-5515/38/3/303

6. Krasheninnikov S, Kukushkin A, Lee W, Phsenov A, Smirnov R, Smolyakov A, et al. Edge and divertor plasma: detachment, stability, and plasma-wall interactions. *Nucl Fusion* (2017) 57:102010. doi:10.1088/1741-4326/aa6d25

7. Angioni C. Impurity transport in tokamak plasmas, theory, modelling and comparison with experiments. *Plasma Phys Controlled Fusion* (2021) 63:073001. doi:10.1088/1361-6587/abfc9a

8. Artaud JF, Imbeaux F, Garcia J, Giruzzi G, Aniel T, Basiuk V, et al. Metis: a fast integrated tokamak modelling tool for scenario design. *Nucl Fusion* (2018) 58:105001. doi:10.1088/1741-4326/aad5b1

9. Bufferand H, Bucalossi J, Ciraolo G, Falchetto G, Gallo A, Ghendrih P, et al. Progress in edge plasma turbulence modelling—hierarchy of models from 2d transport application to 3d fluid simulations in realistic tokamak geometry. *Nucl Fusion* (2021) 61:116052. doi:10.1088/1741-4326/ac2873

10. Reiter D. The eirene code user manual. Julich KFA Report (2005).

11. ITER Physics Expert Group on Confinement and Transport. Plasma confinement and transport. *Nucl Fusion* (1999) 39:2175–249. doi:10.1088/0029-5515/39/12/302

12. Martin YR, Takizuka T. Power requirement for accessing the h-mode in iter. *J Phys Conf Ser* (2008) 123:012033. doi:10.1088/1742-6596/123/1/012033

13. Rivals N. *Understanding density regimes and divertor detachment in ITER relevant conditions. IRFM-CEA Cadarache*. Ph.D. thesis. Aix-Marseille Univeristy (2023).

14. Yang H. *Control of detachment in the divertor region of tokamaks: impact of wall geometry, particle, and energy sources*. Ph.D. thesis. Aix-Marseille University (2023).

15. Bohdansky J. A universal relation for the sputtering yield of monatomic solids at normal ion incidence. *Nucl Instr Methods Phys Res Section B: Beam Interactions Mater Atoms* (1984) 2:587–91. doi:10.1016/0168-583x(84)90271-4

16. Balbinot L, Rubino G, Casiraghi I, Meineri C, Frassinetti L, Aucone L, et al. Multi-code estimation of dtt edge transport parameters. *Nucl Mater Energ* (2023) 34:101350. doi:10.1016/j.nme.2022.101350

17. Faitsch M, Eich T, Harrer G, Wolfrum E, Brida D, David P, et al. Broadening of the power fall-off length in a high density, high confinement h-mode regime in asdex upgrade. *Nucl Mater Energ* (2021) 26:100890. doi:10.1016/j.nme.2020.100890

18. Wesson J, Campbell DJ. *Tokamaks*, 149. Oxford University Press (2011).

19. Balbinot L. *Power exhaust and plasma divertor interaction study by means of a 2D edge numerical code*. Ph.D. thesis. Padova University (2022).

20. Connor J. A review of models for elms. *Plasma Phys control. fusion* (1998) 40:191–213. doi:10.1088/0741-3335/40/2/003